

Detection of Motor Imagery Movements in EEG-based BCI

NIRAJ BAGH, T. JANARDHAN REDDY AND M. RAMASUBBA REDDY

*Biomedical Engineering Group
Department of Applied Mechanics
Indian Institute of Technology
Madras, 600036 India*

E-mail: nirajbagh169@gmail.com; tjanardhanreddy@gmail.com; rsreddy@iitm.ac.in

Motor imagery (MI) based brain-computer interface (BCI) is a communication device that helps motor disabled patients to interact with the surrounding through their brain signals. But, it has low performance due to huge variations of brain patterns among the patients. The main reason behind is that the difference in spatial and temporal distribution of the brain signals. In order to boost the efficiency of the system, this paper combined features obtained from the Hilbert transform (HT) and second order difference plot (SODP). The proposed technique decomposed raw electroencephalogram (EEG) signals into multiple sub-bands with distinct frequency bands. The event-related patterns (ERPs) and MI features for each band were extracted through the HT and SODP. The obtained ERPs and MI features were fed into a multi-class support vector machine (SVM) for decoding brain activities. Two different benchmark datasets (BCI competition-III and IV) were used to evaluate the performance of the proposed method. The results show that the mean classification accuracy (%CA) and Cohen's kappa coefficient (K) obtained from the proposed technique are higher than state-of-the-art techniques.

Keywords: brain computer interface, electroencephalogram, Hilbert transform, second order difference plot, support vector machine

1. INTRODUCTION

The human brain is a complex network that consists of around 100 billion neurons, which are responsible for various activities such as breathing, talking, smelling, *etc.* One of the important activities is communication through voluntary muscle movements. These voluntary muscle movements are controlled by the motor neurons present in motor cortex of the brain. Motor neuron disease (MND) is a neuro-degenerative disorder that damages neurons of the central nervous system (CNS). Amyotrophic lateral sclerosis (ALS) is a common cause of MND, where nerve cells of the brain started dying resulting paralyzed the person [1]. The ALS patients always depended on an assistant thus degrade their quality of life. To enhance their quality of life, they need a technology or communication device which provides alternative communication and control options for ALS patients. One such option is the brain-computer interface (BCI), which acts as an effective communication protocol for motor disabled people.

Received August 14, 2019; revised November 13, 2019; accepted January 2, 2020.
Communicated by Filbert Hilman Juwono.

BCI is a control system that alters brain activities into control signals and acts as a new communication bridge between the ALS patients and outside environment [2]. There are several methods to assess brain activities such as magnetoencephalogram (MEG), near-infrared spectroscopy (NIRS), functional magnetic resonance imaging (fMRI) and electroencephalogram (EEG). However, EEG is commonly used because of high temporal resolution, low cost, portability and non-invasive nature.

There are four distinct kinds of EEG-based BCI system depending on the brain signals such as slow cortical potentials (SCPs), P300 evoked potential (P300), steady-state visual evoked potential (SSVEP) and motor imagery (MI) [3-5]. In recent times, MI-based BCI system draws more attention to the researchers because it doesn't require any external hardware to evoke brain activities. Motor imagery is a procedure where a subject accomplishes a specific task mentally without performing actual voluntary movements. As per literature, when a subject performs any self-paced voluntary movements, the power of μ (8-12 Hz) and β (13-30 Hz) frequency bands start to decrease/increase from/to ideal state. This operation is known as event-related desynchronization (ERD) and event-related synchronization (ERS) [6]. The MI-based BCI includes acquisition of raw EEG signal, pre-processing, feature extraction and detection of brain activities. Feature extraction plays a major role that brings out information of the brain activities corresponding to various voluntary movements. But, the extraction of relevant features from the human brain is a challenging task. In the past, various feature extraction techniques were developed by numerous scientists around the globe. In order to validate their proposed techniques, they have employed two different MI-EEG datasets (BCI competition-III and IV). They have computed classification accuracy (%CA) and Cohen's kappa coefficients (K) and compared their performance with traditional techniques.

Some authors used BCI competition-III dataset and compared their results with existing methods in terms of %CA. For example, Schlogl *et al.* used an adaptive autoregressive (AAR) model to extract information of the brain activities and the activities were detected by minimum distance analysis (MDA) [7]. Hu *et al.* used a hybrid model, *i.e.*, a combination of common average reference (CAR) and common spatial pattern (CSP) to extract new features of the brain patterns [8]. Li *et al.* computed MI features from wavelet packet decomposition (WPD) and the movements were decoded through the support vector machine (SVM) and neural network (NN) [9]. Ge *et al.* implemented a short-time Fourier transform (STFT) and CSP to classify MI movements through the SVM [10]. Shi *et al.* calculated features from sparse CSP and the voluntary movements were identified by the SVM [11]. Meanwhile, Mahmood *et al.* employed four sub-bands (7-13 Hz, 13-19 Hz, 19-25 Hz and 25-31 Hz) and extracted the brain activities using CSP [12]. Some researchers used BCI competition-IV dataset and improved the performance of the BCI system. For instance, Grosse *et al.* discussed the shortcomings of common spatial patterns (CSP) through information-theoretic feature extraction (ITFE) [13]. Zang *et al.* applied Bayesian learning for spatial filtering in EEG-based BCI and introduced the gamma probability model to explain the brain activities [14]. Zanini *et al.* represented the data into a special matrix known as symmetric positive definite (SPD) using Rayleigh geometry [15]. Xi *et al.* extracted MI information by employing SPD matrices obtained from the Riemannian distance [16].

Meanwhile, some researchers have used advanced techniques like common spatial pattern (CSP), filter bank common spatial pattern (FBCSP), regressive analysis (RA) and

independent component analysis (ICA), time frequency-information, multi-segment joint approximate diagonalization (MSJAD) and second order difference plot (SODP) to extract various brain patterns [17-22]. But, satisfying outcomes have been accomplished by some of them. For real-time applications, it is necessary to improve the performance of the system, which is a major issue in MI-based BCI. In order to solve the above issue, first time this article recommends a combination of event-related patterns (ERPs) and second order difference plot (SODP). First, the filter bank technique was implemented to raw EEG signals and multiple numbers of sub-bands were generated. The MI features like ERPs and area of SODP were obtained for each sub-band.

Finally, a multi-class SVM was employed to detect four types of MI activities through the obtained EEG features. The remainder of this paper is organized as follows. Section 2 describes motor imagery-based EEG database. The suggested methodology is illustrated in Section 3. Results and discussion are provided in Section 4. Finally, the paper is concluded in Section 5.

2. MI-EEG DATABASE

In order to evaluate the efficiency of the proposed method, two different benchmark MI-EEG datasets were used. The detailed description of both the datasets were explained in the following sub-sections.

2.1 BCI Competition-III, Dataset-3a

The Neuroscan EEG amplifier was used to record raw data of three subjects (K3b, K6b and L1b). In the experiment, the subjects were given instructions to sit on a chair with armrest. They were informed to imagine four movements (left hand, right hand, feet and tongue) in the direction of a random visual cue. The experiment consists of several runs and each run had 40 trials. The time segment of one trial is 7 s. First, an empty black screen was displayed for 2 s (0 to 2 s), which indicates the beginning of each trial. At $t = 2$ s, a beep sound along with a cross mark was displayed to alert the subject. At $t = 3$ s, an arrow pointing toward left, right, up or down direction was displayed for 1 s. At the same time, the subjects were asked to imagine the movements concerning an arrow direction till $t = 7$ s. The raw signals were measured through 60-channels EEG amplifier where right and left mastoids are served as ground and reference, respectively. The raw signals were filtered between 1 to 50 Hz using a band-pass filter (BPF) and sampled at 250 Hz. The detailed connections of electrodes and visual paradigm were explained in [23].

2.2 BCI Competition-IV, Dataset-2a

The raw EEG signals were recorded from 9 healthy subjects performing four MI movements (left hand, right hand, feet and tongue). The experiments were conducted on different days in two sessions. Each session consists of 6 runs, which included 48 MI trials (12 MI trials for each movement). The time duration of one trial is 7.5 s. A cross mark along with a beep sound was presented from $t = 0$ to 2 s at the initial stage of each trial. At $t = 2$ s, an arrow is directing left, right, up or down direction corresponding to each of the four movements. At $t = 3$ s, the subjects were intimated to imagine respective movements according to direction of an arrow till $t = 6$ s.

A 1.5 s break follows the MI tasks. Twenty-two Ag/AgCl electrodes were used for EEG and three electrodes were used for electrooculogram (EOG) data recording. The raw signals were filtered between 0.5 to 100 Hz using a band-pass filter (BPF). The power line interference was removed by implementing a 50 Hz notch filter and the signals were sampled at 250 Hz. The detailed connections of electrodes and visual paradigm were explained in [24].

3. PROPOSED METHODOLOGY

The detailed steps for decoding MI activities are shown in Fig. 1. In the first step, filter bank technique was employed to decompose each raw EEG signal into sets of six sub-bands (8-12 Hz, 12-16 Hz, 16-20 Hz, 20-24 Hz, 24-28 Hz and 28-32 Hz). In the next step, the HT and SODP were applied to each sub-band and their corresponding MI features were obtained. Finally, the calculated MI features were fed into a multi-class support vector machine to detect various MI activities.

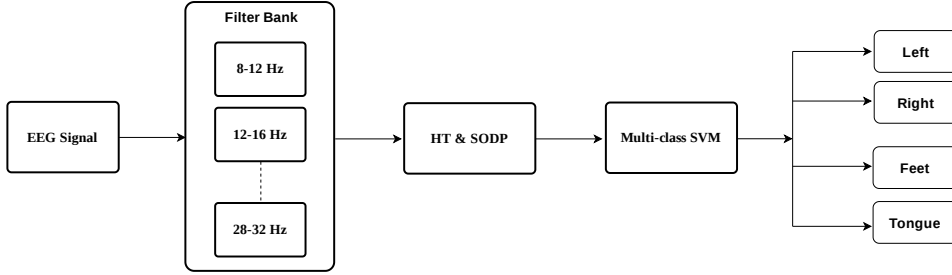


Fig. 1. Steps for decoding MI activities.

3.1 Event-related Patterns using the Hilbert Transform

The band power (BP) plays a vital role in analysis of the brain activities. The average BP of an EEG signal can be calculated using Eq. (1):

$$BP(l) = \frac{1}{N} \sum_{k=1}^N x_{f(k,l)}^2 \quad (1)$$

where $x_{f(k,l)}$ is l^{th} EEG sample in k^{th} trial and N is the total number of MI trials. The event-related pattern (ERP) for various MI activities can be calculated from Eq. (2) :

$$\%ERP(l) = \frac{BP_{event}(l) - BP_{rest}}{BP_{rest}} \times 100\% \quad (2)$$

where BP_{event} and BP_{rest} are the BP of the signals when the subject is performing MI movements and in rest state. The Hilbert transform (HT) uses a phase-shift operator to convert a real signal $x(t)$ into another new signal $x_h(t)$. The obtained new signal has a phase shift of $\pi/2$ radians and it is known as an analytic signal.

The HT of a signal $x(t)$ is calculated from Eq. (3) [25]:

$$x_h(t) = H[x(t)] = \frac{1}{\pi} \int_{-\infty}^{+\infty} \frac{x(\tau)}{t - \tau} d\tau \quad (3)$$

The analytic signal is calculated from Eq. (4):

$$x_a(t) = x(t) + jx_h(t) \quad (4)$$

The envelope of the signal $x_a(t)$ can be obtained from Eq. (5):

$$|x_a(t)| = \sqrt{x(t)^2 + x_h(t)^2} \quad (5)$$

The envelope of the analytic signal helps to identify ERP corresponding to various MI activities. According to Eq. (5), the envelope of event-related patterns can be obtained from Eq. (6):

$$|\%ERP_a(t)| = \sqrt{\%ERP(t)^2 + \%ERP_h(t)^2} \quad (6)$$

where $\%ERP(t)$ is the event-related pattern and $\%ERP_h(t)$ is the HT of event-related pattern for various brain activities.

3.2 Second Order Difference Plot

The second order difference plot (SODP) gives the rate of variation of the successive samples [26]. It can be obtained by plotting $A[n]$ against $B[n]$, which gives a graphical view of the rate of variability between $A[n]$ and $B[n]$ and presented in Eqs. (7) and (8):

$$A[n] = x[n+1] - x[n] \quad (7)$$

$$B[n] = x[n+2] - x[n+1] \quad (8)$$

The shape of SODP pattern is elliptical and therefore area of the ellipse can be used as a feature to detect various MI activities. The 95% confidence area of the ellipse can be used to quantify four types of MI tasks [27]. In order to obtain area of the ellipse, variance of $A[n]$, $B[n]$ and the covariance between $A[n]$ and $B[n]$ were calculated using Eqs. (9)-(11):

$$\sigma_A = \sqrt{\frac{1}{M} \sum_{n=0}^{M-1} A[n]^2} \quad (9)$$

$$\sigma_B = \sqrt{\frac{1}{M} \sum_{n=0}^{M-1} B[n]^2} \quad (10)$$

$$\sigma_{AB} = \frac{1}{M} \sum_{n=0}^{M-1} A[n]B[n] \quad (11)$$

where σ_A^2 , σ_B^2 , σ_{AB}^2 are the variance of A, B and covariance between A and B. M is the total number of sample points. The diameter (D), major axis (a) and minor axis (b) of the ellipse can be obtained from Eqs. (12)-(14):

$$D = \sqrt{(\sigma_A^2 + \sigma_B^2) - 4(\sigma_A^2 \sigma_B^2 - \sigma_{AB}^2)} \quad (12)$$

$$a = 1.7321 \sqrt{(\sigma_A^2 + \sigma_B^2 + D)} \quad (13)$$

$$b = 1.7321 \sqrt{(\sigma_A^2 + \sigma_B^2 - D)} \quad (14)$$

Finally, area of the ellipse can be calculated from Eq. (15):

$$Area = \pi ab. \quad (15)$$

3.3 Support Vector Machine

The support vector machine (SVM) is a powerful machine learning model that constructs an optimal line or hyperplane to separate points between two classes or among the multiple classes. It separates points by finding weight vector and bias of the hyperplane [28, 29]. The performance of the SVM was evaluated by classification accuracy (%CA), precision (P), sensitivity (S), F1-score and Cohen's kappa coefficient (K). The model parameters can be obtained from Eqs. (16)-(20):

$$\%CA = \frac{TP + TN}{TP + FN + FP + TN} \times 100\% \quad (16)$$

$$P = \frac{TP}{TP + FP} \quad (17)$$

$$S = \frac{TP}{TP + FN} \quad (18)$$

$$F1 - score = 2 \left(\frac{P \times S}{P + S} \right) \quad (19)$$

$$K = \frac{CA - \frac{1}{N_c}}{1 - \frac{1}{N_c}} \quad (20)$$

where TP is true positive that correctly predicted MI-EEG trials. FP is false positive that incorrectly predicted MI-EEG trials. TN is true negative that correctly rejected MI-EEG trials. FN is false negative that incorrectly rejected MI-EEG trials. N_c is the number of classes.

4. RESULTS AND DISCUSSION

The raw signals obtained from C3, Cz and C4 channels were decomposed by filter bank technique and multiple numbers of sub-bands were generated. Fig. 2 shows signal of one sub-band, *i.e.*, μ band (8 – 12 Hz) in three channels for BCI competition-III dataset. Figs. 2 (i)-(iv) represent variation in the μ band while the subject is performing four different MI tasks. In order to analyze deeper, the ERPs were extracted through the Hilbert

transform. Fig. 3 illustrates $\%ERP_a$ for all MI activities in three channels. Fig. 3 (i) shows the variation of the patterns in three channels when the subject is performing left hand MI movement. As we know that the C3 and C4 channels are placed over left and right hemispheres of the brain. When the subject is imagining left hand MI movement, then the pattern in C4 channel starts decreasing. During MI period, the pattern in C4 channel is lower than C3 channel which indicates that the ERD activity is occurring in C4 channel. Meanwhile, the ERS activity is observing in C3 channel.

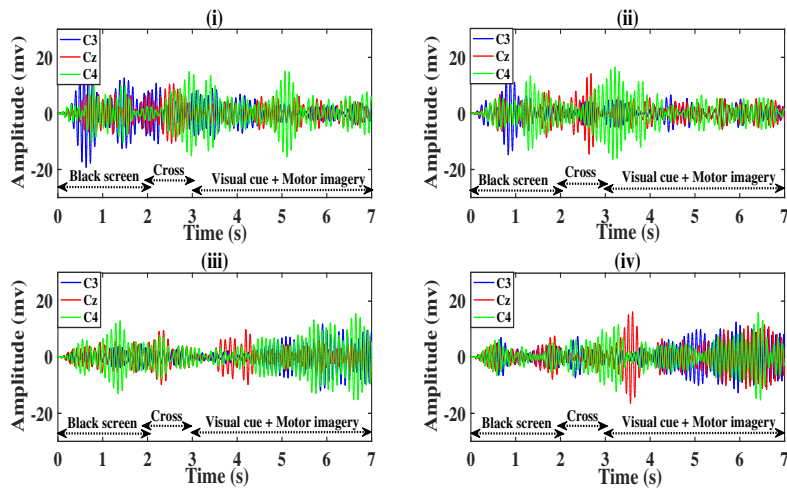


Fig. 2. EEG signals obtained from BCI competition-III dataset during (i) left hand; (ii) right hand; (iii) feet and (iv) tongue MI movements.

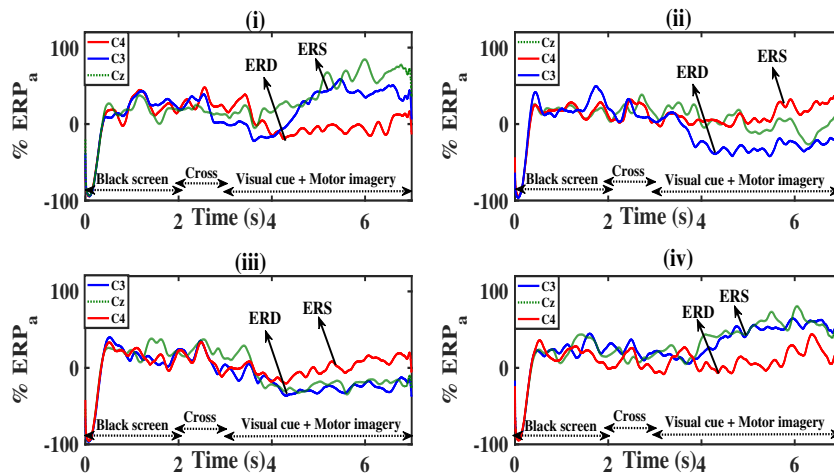


Fig. 3. ERPs for BCI competition-III dataset during (i) left hand; (ii) right hand; (iii) feet and (iv) tongue MI movements.

This decreasing in the pattern is due to desynchronization of motor neurons in the right hemisphere of the brain. It implies that the motor neurons present in right hemisphere of the brain are responsible for controlling left-hand MI movement. Fig. 3 (ii) shows the variation of the patterns in three channels when the subject is performed right-hand MI movement. During MI period, the pattern in C3 channel is lower than C4 channel. This indicates that the ERD process is occurring in C3 channel and the ERS activity is observing in C4 channel. It inferred that the motor neurons present in left hemisphere of the brain are responsible for controlling right hand MI movement. Similarly, Figs. 3 (iii) & (iv) reveal that when the subject is performing both feet and tongue MI movements, then variation of the patterns were observed in three channels. The variation of the patterns demonstrated that the MI activities are effectively captured in three channels. In order to study the non-linear dynamical behavior of the signal, SODP was applied to each sub-band. It gives the rate of variability or chaos in three channels when the subject is performing various MI movements.

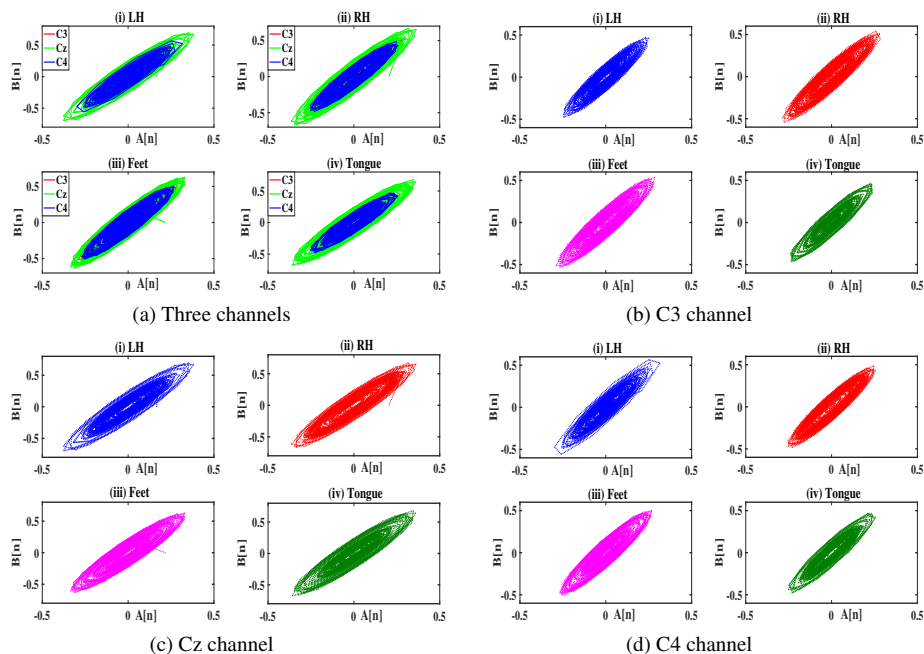


Fig. 4. SODP patterns for BCI Competition-III dataset during (i) left hand; (ii) right hand; (iii) feet and (iv) tongue MI movements.

Fig. 4 illustrates SODP patterns for all MI activities in three channels for BCI competition-III dataset. Fig. 4 (a) shows the variation of SODP patterns in three channels when the subject is performing four MI activities. But, the variation of the patterns in three channels are not clearly noticeable in the figure. Therefore, SODP patterns for each MI movement were calculated in three individual channels and plotted in Figs. 4 (b)-(d). Each figure has four subplots, where subplots (i), (ii), (iii) & (iv) represent SODP patterns in left hand, right hand, feet and tongue movements, respectively.

Table 1. Model parameters for both BCI competition-III and IV datasets.

BCI-Competition-III, Dataset-3a															
Subjects	Case-1, ERPs					Case-2, Area					Case-3, ERPs+Area				
	%CA	P	S	F1-score	K	%CA	P	S	F1-score	K	%CA	P	S	F1-score	K
K3b	82.70	0.83	0.83	0.83	0.76	92.70	0.93	0.93	0.93	0.90	95.00	0.95	0.95	0.95	0.93
K6b	73.33	0.74	0.73	0.73	0.64	74.16	0.74	0.74	0.74	0.65	89.16	0.90	0.89	0.89	0.85
L1B	72.50	0.73	0.72	0.72	0.63	87.50	0.88	0.88	0.87	0.83	93.33	0.94	0.93	0.93	0.91
Mean	76.17	0.76	0.76	0.76	0.67	84.78	0.85	0.85	0.84	0.79	92.49	0.93	0.92	0.92	0.89
BCI-Competition-IV, Dataset-2a															
S1	93.75	0.94	0.94	0.94	0.91	95.13	0.96	0.95	0.95	0.93	85.40	0.86	0.85	0.85	0.80
S2	56.25	0.56	0.56	0.56	0.41	67.56	0.68	0.68	0.68	0.56	79.93	0.80	0.80	0.80	0.73
S3	75.00	0.75	0.75	0.75	0.66	94.07	0.94	0.94	0.94	0.92	95.13	0.96	0.95	0.96	0.92
S4	87.50	0.88	0.88	0.87	0.83	88.19	0.88	0.88	0.88	0.84	98.61	0.99	0.98	0.99	0.98
S5	88.88	0.89	0.89	0.89	0.85	92.01	0.92	0.92	0.92	0.89	95.30	0.96	0.96	0.96	0.93
S6	74.30	0.74	0.74	0.74	0.65	83.40	0.84	0.83	0.83	0.77	84.40	0.84	0.83	0.83	0.77
S7	79.86	0.80	0.80	0.81	0.73	88.61	0.89	0.89	0.89	0.84	84.72	0.85	0.85	0.85	0.79
S8	75.34	0.78	0.75	0.75	0.67	90.67	0.91	0.91	0.91	0.87	85.13	0.86	0.85	0.85	0.80
S9	85.13	0.85	0.85	0.86	0.80	88.54	0.89	0.89	0.88	0.84	87.92	0.88	0.88	0.88	0.83
Mean	79.55	0.79	0.79	0.79	0.72	87.57	0.87	0.87	0.87	0.82	88.39	0.88	0.88	0.88	0.83

The obtained SODP patterns are elliptical and their sizes are distinct for different MI movements. These distinct sizes of the patterns are due to presence of chaotic behavior during MI period. The changes in the area of ellipse, indicating that the SODP is playing a significant role and captured the chaotic behavior of the signal. Hence, area of the ellipse can be used as a feature to discriminate four different MI tasks. The MI features obtained from both the HT and SODP were combined and fed into a multi-class support vector machine and the performance of the model was evaluated for both the datasets. The performance of the SVM was evaluated by considering three special cases. The ERPs and area of the ellipse were considered as feature vectors in case-(1) and case-(2), respectively.

The features obtained from case-(1) and case-(2) were combined and considered as a case-(3). The performance (%CA, P, S, F1-score and K) of the model in three different cases was evaluated and listed in Table 1. It is observed that the performance of case-(3) is superior to the remaining two cases in both the datasets. In case-(3), the %CA and K for both BCI competition-III and IV datasets were found to be 92.49% & 0.89 and 88.39% & 0.83, respectively. Case-(3) of the proposed method gives better result and therefore it was taken into consideration while comparing with several existing methods. Table 2 compares the performance of the proposed method with existing methods in terms of %CA. The mean %CA of all three subjects was found to be 92.49% which is higher than the existing methods on BCI competition-II dataset. The highest and lowest %CA, *i.e.*, 95.00% & 89.16% were found in K3b and K6b subjects. Table 3 compares the performance of the proposed method with conventional methods in terms of %CA.

Table 2. Comparison between the proposed and conventional methods on BCI competition-III, dataset-3a.

Proposed by	Feature extraction	Classifier	%CA			Mean
			K3b	K6b	L1b	
Schlogl <i>et al.</i> [7]	Adaptive auto-regressive model	MDA	66.60	38.50	49.50	51.50
Hu <i>et al.</i> [8]	Combination of CAR and CSP	NN	41.60	41.70	49.50	44.26
Li <i>et al.</i> [9]	WPD	SVM+NN	83.10	84.40	85.60	84.40
Ge <i>et al.</i> [10]	Combination of STFT and CSP	SVM	71.30	88.10	71.20	76.90
Shi <i>et al.</i> [11]	Sparse PCA+CSP	SVM	85.10	81.60	80.10	82.30
Mahmood <i>et al.</i> [12]	Four sub-bands CSP	SVM	93.30	77.50	85.80	85.50
Present	Proposed	SVM	95.00	89.16	93.33	92.49

Table 3. Comparison between the proposed and conventional methods on BCI competition-IV, dataset-2a.

Subjects	Gross <i>et al.</i> [13]	Zhang <i>et al.</i> [14]	Zanini <i>et al.</i> [15]	CSP+LDA [16]	CSP+SVM [16]	Proposed
S1	48.10	61.50	77.80	78.30	76.30	85.40
S2	27.30	32.10	44.10	44.70	50.70	79.93
S3	70.60	68.60	76.80	82.20	85.10	95.13
S4	21.40	27.10	54.90	59.10	52.90	98.61
S5	22.70	34.30	43.80	39.70	48.80	95.30
S6	32.40	35.30	47.10	50.10	49.20	83.40
S7	52.30	48.00	72.00	81.00	78.10	84.72
S8	65.80	65.60	75.20	68.50	77.40	85.13
S9	34.20	41.80	76.60	77.40	82.20	87.92
Mean	41.64	46.01	63.20	64.60	66.70	88.39

Table 4. Comparison between the proposed and conventional methods on BCI competition-IV, dataset-2a.

Subjects	Ang <i>et al.</i> [17]	Liu <i>et al.</i> [18]	Wang <i>et al.</i> [19]	Kam <i>et al.</i> [20]	Pailler <i>et al.</i> [21]	Bagh <i>et al.</i> [22]	Proposed
S1	0.68	0.69	0.56	0.74	0.66	0.59	0.80
S2	0.42	0.34	0.41	0.35	0.42	0.77	0.73
S3	0.75	0.71	0.43	0.76	0.77	0.73	0.92
S4	0.48	0.44	0.41	0.53	0.51	0.35	0.98
S5	0.40	0.16	0.68	0.38	0.50	0.63	0.93
S6	0.27	0.21	0.48	0.31	0.21	0.56	0.77
S7	0.77	0.66	0.80	0.84	0.30	0.61	0.79
S8	0.75	0.73	0.72	0.74	0.69	0.51	0.80
S9	0.61	0.69	0.63	0.60	0.46	0.81	0.83
Mean	0.57	0.52	0.57	0.60	0.50	0.62	0.83

The mean %CA of all nine subjects was found to be 88.39% which is superior to state-of-the-art methods. The highest and lowest values of %CA, *i.e.*, 98.61% & 79.93% were found in S4 and S2 subjects. Similarly, Table 4 compares the performance of the proposed method with conventional methods in terms of K . The mean value of K for all nine subjects was found to be 0.83 which is higher than the existing methods. The highest and lowest values of K , *i.e.*, 0.98 & 0.73 were found in S4 and S2 subjects. The maximum and minimum values of %CA and K represent the sensitivity of the subjects toward MI tasks. The maximum value shows high sensitivity of the subject whereas minimum value reveals the subject is not performing MI tasks properly and it is known as BCI illiteracy.

5. CONCLUSIONS

In this research, the event-related patterns and areas of the ellipses are used to detect various MI activities of the subjects. The event-related patterns are identified by the Hilbert transform, whereas areas of the ellipses are obtained from the second order difference plot. Two approaches have been employed to discriminate four different MI tasks: one is graphical and the other is machine learning. The graphical method shows that the event-related patterns and shapes of the ellipses are changing when the subject is performing MI movements. In the machine learning approach, the event-related patterns and areas of the ellipses are used as features to classify MI movements. The performance is higher when combined event-related patterns and areas of the ellipses. Both the Hilbert transform and the second order difference plot contributed significant MI features, which helps to boost the efficiency of the system. Finally, the efficiency of the proposed method was compared with several existing methods and results show that the presented method outperformed state-of-the-art methods.

ACKNOWLEDGMENT

The authors would like to thank R. Leeb, C. Brunner, G.R Muller-Purtz, A. Schlogl and G. Pfurtscheller for providing the MI EEG data of BCI Competition-III and IV.

REFERENCES

1. M. Hecht, *et al.*, "Subjective experience and coping in ALS," *Amyotrophic Lateral Sclerosis and Other Motor Neuron Disorders*, Vol. 3, 2002, pp. 225-231.
2. J. R. Wolpaw, *et al.*, "Brain-computer interfaces for communication and control," *Clinical Neurophysiology*, Vol. 113, 2002, pp. 767-791.
3. T. J. Bradberry, R. J. Gentili, and J. L. Contreras-Vidal, "Reconstructing three-dimensional hand movements from noninvasive electroencephalographic signals," *Journal of Neuroscience*, Vol. 30, 2010, pp. 3432-3437.
4. J. D. Bayliss and D. H. Ballard, "A virtual reality testbed for brain-computer interface research," *IEEE Transactions on Rehabilitation Engineering*, Vol. 8, 2000, pp. 188-190.
5. N. Birbaumer, *et al.*, "A spelling device for the paralysed," *Nature*, Vol. 398, 1999, p. 297.
6. G. Pfurtscheller, C. Neuper, D. Flotzinger, and M. Pregenzer, "Eeg-based discrimination between imagination of right and left hand movement," *Clinical Neurophysiology*, Vol. 103, 1997, pp. 642-651.
7. A. Schlögl, F. Lee, H. Bischof, and G. Pfurtscheller, "Characterization of four-class motor imagery eeg data for the bci-competition 2005," *Journal of Neural Engineering*, Vol. 2, 2005, p. L14.
8. J. F. Hu, Z. D. Mu, and J. H. Yin, "Features extraction method of motor imagery eeg based on information granules," in *Applied Mechanics and Materials*, Vol. 496, 2014, pp. 1982-1985.

9. M. Li, L. Lin, and S. Jia, "Multi-class imagery eeg recognition based on adaptive subject-based feature extraction and svm-bp classifier," in *Proceedings of IEEE International Conference on Mechatronics and Automation*, 2011, pp. 1184-1189.
10. S. Ge, R. Wang, and D. Yu, "Classification of four-class motor imagery employing single-channel electroencephalography," *PloS One*, Vol. 9, 2014, p. e98019.
11. L.-C. Shi, Y. Li, R.-H. Sun, and B.-L. Lu, "A sparse common spatial pattern algorithm for brain-computer interface," in *Proceedings of International Conference on Neural Information Processing*, 2011, pp. 725-733.
12. A. Mahmood, R. Zainab, R. B. Ahmad, M. Saeed, and A. M. Kamboh, "Classification of multi-class motor imagery eeg using four band common spatial pattern," in *Proceedings of the 39th Annual International Conference of IEEE Engineering in Medicine and Biology Society*, 2017, pp. 1034-1037.
13. M. Grosse-Wentrup and M. Buss, "Multiclass common spatial patterns and information theoretic feature extraction," *IEEE Transactions on Biomedical Engineering*, Vol. 55, 2008, pp. 1991-2000.
14. H. Zhang, H. Yang, and C. Guan, "Bayesian learning for spatial filtering in an eeg-based brain-computer interface," *IEEE Transactions on Neural Networks and Learning Systems*, Vol. 24, 2013, pp. 1049-1060.
15. P. Zanini, M. Congedo, C. Jutten, S. Said, and Y. Berthoumieu, "Transfer learning: a riemannian geometry framework with applications to brain-computer interfaces," *IEEE Transactions on Biomedical Engineering*, Vol. 65, 2018, pp. 1107-1116.
16. X. Xie, *et al.*, "Motor imagery classification based on bilinear sub-manifold learning of symmetric positive-definite matrices," *IEEE Transactions on Neural Systems and Rehabilitation Engineering*, Vol. 25, 2017, pp. 504-516.
17. K. K. Ang, *et al.*, "Filter bank common spatial pattern algorithm on bci competition iv datasets 2a and 2b," *Frontiers in Neuroscience*, Vol. 6, 2012, p. 39.
18. H. G. Liu Guangquan, "Bci competition-iv results," <http://www.bbci.de/competition/iv/results/>, 2008.
19. D. Wang, D. Miao, and G. Blohm, "Multi-class motor imagery eeg decoding for brain-computer interfaces," *Frontiers in Neuroscience*, Vol. 6, 2012, p. 151.
20. T.-E. Kam, H.-I. Suk, and S.-W. Lee, "Non-homogeneous spatial filter optimization for electroencephalogram (eeg)-based motor imagery classification," *Neurocomputing*, Vol. 108, 2013, pp. 58-68.
21. C. Gouy-Pailler, M. Congedo, C. Brunner, C. Jutten, and G. Pfurtscheller, "Nonstationary brain source separation for multiclass motor imagery," *IEEE Transactions on Biomedical Engineering*, Vol. 57, 2010, pp. 469-478.
22. N. Bagh and M. R. Reddy, "Second order difference plot to decode multi-class motor imagery activities," in *Proceedings of the 7th International Conference on Smart Computing and Communications*, 2019, pp. 1-4.
23. B. Blankertz, *et al.*, "The bci competition iii: Validating alternative approaches to actual bci problems," *IEEE Transactions on Neural Systems and Rehabilitation Engineering*, Vol. 14, 2006, pp. 153-159.
24. G. Pfurtscheller, "Graz description of data set iv of bci competition," <http://www.bbci.de/competition/iv/>, 2008.
25. N. Thrane, "The hilbert transform," *B&K Technical Review*, Vol. 3, 1984, pp. 3-15.

26. M. Brennan, M. Palaniswami, and P. Kamen, "Do existing measures of poincare plot geometry reflect nonlinear features of heart rate variability?" *IEEE Transactions on Biomedical Engineering*, Vol. 48, 2001, pp. 1342-1347.
27. T. E. Prieto, J. B. Myklebust, R. G. Hoffmann, E. G. Lovett, and B. M. Myklebust, "Measures of postural steadiness: differences between healthy young and elderly adults," *IEEE Transactions on Biomedical Engineering*, Vol. 43, 1996, pp. 956-966.
28. V. Vapnik, *The Nature of Statistical Learning Theory*, Springer Science & Business Media, NY, 2013.
29. R. O. Duda, P. E. Hart, and D. G. Stork, *Pattern Classification*, John Wiley & Sons, US, 2012.



Niraj Bagh is currently pursuing Ph.D. at Indian Institute of Technology, Madras. His research area is motor imagery-based brain computer interface. His research aim is to decode different brain activities using various non-linear feature extraction techniques along with machine learning and deep learning models.



T. Janardhan Reddy is currently pursuing Ph.D. at Indian Institute of Technology, Madras. His research area is biomedical signal processing. He is a member of IEEE and IETE. He worked as an Assistant Professor at various private organizations in India.



M. Ramasubba Reddy is a Senior Professor in Biomedical Engineering Group, Department of Applied Mechanics, Indian Institute of Technology, Madras. His research and teaching focus on Biomedical Instrumentation, Signal and Image Processing, Rehabilitation Engineering and Physiological Modeling. He holds a Ph.D. from Indian Institute of Science, Bangalore, India and served as the Head of Biomedical Engineering Group, Applied Mechanics Department at IIT Madras for more than six years.